The Canadian Mineralogist
Vol. 50, pp. 253-265 (2012)
DOI: 10.3749/canmin.50.2.253

THE CRYSTAL STRUCTURE OF GUETTARDITE, $PbAsSbS_4$, AND THE TWINNITE–GUETTARDITE PROBLEM

Emil MAKOVICKY[§]

Department of Geography and Geology, University of Copenhagen, Østervoldgade 10, DK–1350 Copenhagen K, Denmark

Dan TOPA

Department of Materials Research and Physics, Paris–Lodron University of Salzburg, Hellbrunnerstrasse 34,
A–5020 Salzburg, Austria

Husein TAJJEDIN and Ebrahim RASTAD

Department of Geology, Faculty of Basic Sciences, Tarbiat Modares University, P.O. Box 14115–175, Tehran, Iran

Abdolmajid YAGHUBPUR

Department of Geology, Tarbiat Moallem University, Tehran, Iran

Abstract

Guettardite from the Barika Au–Ag deposit in Azarbaijan Province, western Iran, formed in fractures developed in silica bands situated in massive banded pyrite and barite ores. Fractures host veinlets that contain a number of Ag–As–Sb–Pb-rich sulfosalts, tetrahedrite–tennantite, realgar, pyrite and Au–Ag alloy. The variation in the chemical composition of guettardite is minor: $Pb_{0.95–0.96}Sb_{0.96–1.02}As_{1.03–1.06}S_{3.99–4.02}$. The lattice parameters were determined from a single crystal as a 8.527(4), b 7.971(4), c 20.102(10) Å, β 101.814(7)°, space group $P2_1/c$. The structure of guettardite contains six distinct coordination polyhedra of cations. Atoms Pb1 and Pb2 form slightly skewed tricapped trigonal coordination prisms arranged in a zig-zag layer. Two distinct As and two Sb sites in a chess-board arrangement form MeS_5 pyramids with trapezoidal bases. Guettardite is a homologue of sartorite, ideally $PbAs_2S_4$, and is the N = 3 member of the sartorite homologous series of sulfosalts. We contend that guettardite and twinnite are configurational polytypes composed of two alternating types of OD layers, formed by different orientations of tightly bonded crankshaft chains in adjacent As–Sb-based OD layers (layer symmetry $P\bar{1}$) separated by a Pb-based OD layers [layer symmetry $Pm2_1(n)$]. Whether the observed differences in the Sb:As ratio determine the polytype is still an open question. A complete structural analogy has been found in the pair $BaSb_2S_4$ – $BaSb_2Se_4$.

Keywords: guettardite, sulfosalt, crystal structure, polytype, OD layers, Barika deposit, Iran.

Introduction

Guettardite was described by Jambor (1967a) from a prospect pit excavated in marble at Madoc, Huntington Township, Ontario, as a monoclinic sulfosalt with a formula $Pb(Sb_{1.12}As_{0.88})_{\Sigma 2}S_4$. The description brought about an immediate problem because he also defined twinnite $Pb(Sb_{1.26}As_{0.74})_{\Sigma 2}S_4$ as an orthorhombic sulfosalt from the same deposit. Guettardite (and twinnite) are the lowermost (N = 3) known members of the sartorite homologous series (Makovicky 1985, Berlepsch *et al*. 2001a, Moëlo *et al*. 2008), and are homeotypes of the arsenian sulfosalt, sartorite (Nowacki *et al*. 1961, Iitaka & Nowacki 1961, Berlepsch *et al*. 2003). They also are representatives of the As–Sb subset of this series, alongside with veenite, $Pb_2(Sb,As)_2S_5$ (Jambor 1967b), which is an N = 4 homologue. At present, the structure of guettardite is unknown. It is assumed that in guettardite, the regular distribution of As and Sb over the metalloid positions results in a better fit with the lead-rich portions of the structure, and commensurability along the n × 4 Å direction is achieved for the 8.7 Å cell without need for complicated bonding sequences and huge supercells observed in nearly pure sartorite, $PbAs_2S_4$. Elucidation of this situation is one of the purposes of the present study.

[§] *E-mail address*: emilm@geo.ku.dk

PREVIOUS INVESTIGATIONS

Occurrences of mixed, antimonian–arsenian homologues of sartorite are infrequent: Madoc, Ontario (Jambor 1967b), Jas Roux, Mont Pelvoux, Hautes-Alpes (Mantienne 1974), the Pitone marble quarry, Seravezza, Tuscany (Bracci *et al.* 1980), further mentions in Kyrgyzstan and Silverton, Colorado (www.mindat.org), and a recently described occurrence at Zarshouran, northwestern Iran (Paar *et al.* 2009). Arsenic-rich "guettardite" (Sb/As ~0.33) has been reported by Ciobanu *et al.* (2005) from Săcărimb, Romania. To these occurrences, we add the present locality, the Barika Au–Ag deposit in the Azarbaijan Province, western Iran. The find of an untwinned single-crystal grain of guettardite from this locality enabled us to determine and refine its crystal structure.

PROVENANCE

The Barika ore deposit is a gold-rich volcanogenic massive sulfide deposit of Cretaceous age, in the metamorphic Sanandaj–Sirjan Zone that stretches as a northwest–southeast zone in the western part of Azarbaijan Province. The greenschist metamorphism and deformation in form of shear zones overprinted the still clearly recognizable synvolcanic stratiform textures. Metamorphism produced a granoblastic texture of pyrite, and ductile deformation resulted in folding, recrystallization and boudinage.

Massive to semimassive banded pyrite and barite ores accompanied by locally developed silica bands form a lens-like deposit approximately 150 m long and up to 20 m thick. Pyrite, sphalerite, galena, tetrahedrite–tennantite and stibnite were deposited during the synvolcanogenic hydrothermal activity. Brittle deformation, fractured porphyroblasts of pyrite and, in addition the silica bands modified the original situation. Fractures host veinlets that contain, among other minerals, a number of Ag–As–Sb–Pb-rich sulfosalts: tetrahedrite–tennantite, stephanite, pyrargyrite, trechmannite, smithite, miargyrite, andorite, geocronite, seligmannite, guettardite and, in addition, realgar, pyrite and a Au–Ag alloy. The chemical remobilization of the components originally housed by the stratiform ores, which led to these minerals, took place at the margins of the orebody. They produced economically important concentrations of recoverable gold in form of a Au–Ag alloy.

The specimen that yielded guettardite is a portion of a quartz vein with irregular thin veinlets and nests of sulfosalts in the mass of quartz: Zn–Hg-bearing tennantite, miargyrite, pyrargyrite, andorite and guettardite.

CHEMICAL COMPOSITION

Guettardite and the associated sulfosalt minerals were analyzed using a JEOL Superprobe JXA–8600 electron microprobe, controlled by PROBE FOR WINDOWS system of programs, and operated at 25 kV and 35 nA, with a beam diameter of 5 μm. Wavelength-dispersion data were collected using the following standards and emission lines: Bi_2S_3 (Bi*L*α), galena (Pb*M*α), chalcopyrite (Cu*K*α, Fe*K*α), Ag metal (Ag*L*α), Sb_2S_3 (Sb*L*α, S*K*α), and InAs (As*L*α). The raw data were corrected with the on-line ZAF–4 procedure. The results of the electron-microprobe analyses are compiled in Table 1. Iron, copper, bismuth, and silver are absent in guettardite. The empirical formulae of guettardite were calculated on the basis of seven atoms per formula unit (*apfu*). The chemical compositions of associated sulfosalt minerals are not presented here and will be discussed in detail in a future paper.

The variation of chemical composition is minor: $Pb_{0.95–0.96}Sb_{0.96–1.02}As_{1.03–1.06}S_{3.99–4.02}$. The deficit in Pb is an analytical artefact. Analyses of the original guettardite from Madoc (Jambor 1967a) indicate problematic $Pb_{1.22}Sb_{1.03}As_{0.95}S_{3.81}$ and $Pb_{1.24}Sb_{1.06}As_{0.94}S_{3.76}$ compositions, respectively, chiefly because of inadequate correction-programs in the early years of electron-microprobe analysis. Jambor *et al.* (1982) reanalyzed this material, and their new electron-microprobe data indicate compositions from $Pb_{1.02}Sb_{1.11}As_{0.81}S_{4.06}$ to $Pb_{1.01}Sb_{1.07}As_{0.88}S_{4.05}$, *i.e.*, with Sb:As ratio between 1.37 and 1.22, broader than and different from the original range, 1.08–1.13. The Tuscany material analyzed by Bracci *et al.* (1980) is $Pb_{1.00}Cu_{0.04}Sb_{1.04}As_{0.98}S_{3.94}$, whereas the Săcărimb "guettardite" yielded microprobe-derived compositions in the range $Pb_{1.02–1.23}Cu_{0.0–0.03}As_{1.26–1.37}Sb_{0.61–0.65}(S,Se)_{3.90–3.93}$ (Ciobanu *et al.* 2005). For Zarshouran, Paar *et al.* (2009) indicated both a material with Sb:As ratio close to 0.90, although with a deficit in lead, analyzed as $Pb_{8.9}Sb_{10.3}As_{11.4}S_{44.2}$, and a material compositionally close to the Săcărimb occurrence, $Pb_{0.94}Cu_{0.01}As_{1.25}Sb_{0.73}S_{4.07}$, possibly an independent mineral species with the Sb:As ratio of only 0.58. Jambor *et al.* (1982) did not indicate to what degree their restudied guettardite material was covered by parallel X-ray powder diffraction. In the absence of proofs to the contrary, we assume here that the typical guettardite assumes the Sb:As ratio close or equal to 1:1.

TABLE 1. AVERAGE RESULTS OF ELECTRON-MICROPROBE ANALYSES OF GUETTARDITE FROM THE BARIKA DEPOSIT, IRAN

Grain	*n*	Pb	As	Sb	S	Total
1	11	37.63(17)	14.97(21)	22.78(74)	24.36(17)	99.74(87)
2	2	37.51(6)	14.89(3)	21.88(4)	24.19(1)	98.46(1)
3	6	37.74(15)	15.08(14)	22.55(28)	24.35(17)	99.72(65)
4	3	37.48(9)	14.82(25)	23.85(26)	24.48(14)	100.63(22)

Compositions are reported in wt.%; *n* number of point analyses. The empirical formulae were calculated on the basis of *Me* + S = 7 *apfu*:
1) $Pb_{0.95}As_{1.05}Sb_{0.98}S_{4.01}$
2) $Pb_{0.96}As_{1.06}Sb_{0.96}S_{4.02}$
3) $Pb_{0.95}As_{1.05}Sb_{0.97}S_{4.02}$
4) $Pb_{0.95}As_{1.03}Sb_{1.02}S_{3.99}$.

The 1982 study changes the formula suggested for twinnite by Jambor (1967a), resulting in a new Sb:As ratio of 1.49–1.94. He also tentatively suggested that X-ray powder-diffraction results from synthetic runs made in the system Pb–As–Sb–S at 400–500°C indicate formation of both guettardite and twinnite (Jambor 1968).

X-Ray-Diffraction Data

For our single-crystal investigation, irregular, blade-like fragments were extracted from the polished specimen. Intensity data were collected on a Bruker AXS P3 diffractometer operated at 50 kV and 35 mA, equipped with a CCD area detector using graphite-monochromated Mo$K\alpha$ radiation. Experimental data are listed in Table 2. The SMART (Bruker AXS 1998a) system of programs was used for unit-cell determination and data collection, SAINT+ (Bruker AXS 1998b) for the reduction of the intensity data, and XPREP (Bruker AXS 1997) for space-group determination and empirical absorption correction based on pseudo Ψ-scans. The centrosymmetric space-group $P2_1/c$, proposed by the XPREP program, was chosen. It is consistent with the monoclinic symmetry of the lattice and intensity statistics (mean $|E^*E - 1| = 0.911$ [expected values: 0.968 for the centrosymmetric case and 0.736 for the non-centrosymmetric case]). The structure of guettardite was solved by direct methods (program SHELXS, Sheldrick 1997a), which revealed the positions of most of the atoms. In subsequent cycles of the refinement (program SHELXL, Sheldrick 1997b), remaining atom-positions were deduced from difference-Fourier syntheses by selecting from among the strongest maxima at appropriate distances.

TABLE 2. SINGLE-CRYSTAL X-RAY DIFFRACTION OF GUETTARDITE: EXPERIMENTAL AND REFINEMENTS DETAILS

Crystal data	
Chemical formula	$PbAsSbS_4$
Formula weight	4256.8
Unit-cell parameters	
a, *b*, *c* (Å)	8.527(4), 7.971(4), 20.102(10)
α, β, γ (°)	90.00, 101.814(7), 90.00
V (Å^3)	1337.3(11)
Crystal system	monoclinic
Space group	$P2_1/c$ (#14)
D_x (g cm^{-3})	5.29
No. of reflections for cell parameters	2526
μ (mm^{-1})	35.22
Z	8
Crystal morphology	irregular
Crystal color	grey metallic
Crystal size (mm)	0.05 × 0.06 × 0.15
Data collection	
T_{min}, T_{max}	0.198, 0.384
No. of measured reflections	5845
No. of independent reflections	1264
No. of observed reflections	1102
Criterion for observed reflections	$F_o > 4\sigma(F_o)$
R_{int}, R_{sigma} (%)	7.5, 4.5
θ_{max} (°)	20.9
Range of *h, k, l*	$-8 \leq h \leq 8$, $-7 \leq k \leq 8$, $-20 \leq l \leq 20$
Refinement	
Refinement on F_o^2	
R [$F_o > 4\sigma(F_o)$] (%)	5.83
wR (F_o^2) (%)	6.66
S (GooF)	1.09
No. of reflections used in refinement	1101
No. of parameters refined	132
Weighting scheme: a = 0.0364, b = 150.97, $w = 1/[\sigma^2(F_o^2) + (aP)^2 + bP]$, where $P = (F_o^2 + 2F_c^2)/3$	
$(\Delta/\sigma)_{max}$	0.001
$\Delta\rho_{max}$ (e/Å^3)	1.83 (1.01 Å from Sb2)
$\Delta\rho_{min}$ (e/Å^3)	-1.75 (1.10 Å from Pb2)
Extinction coefficient	0.00002(7)
Source of atomic scattering factors	*International Tables for X-Ray Crystallography* (1992, Vol. C, Tables 4.2.6.8 and 6.1.1.4)
Computer programs	
Structure solution	*SHELXS97* (Sheldrick 1997a)
Structure refinement	*SHELXL97* (Sheldrick 1997b)

The structure of guettardite contains six distinct coordination-polyhedra of cations and eight of anions. In the final stage of refinement, all positions were treated as anisotropic, and the occupancy of the Sb and As sites was left free. Data on X-ray diffraction and the structure refinement are summarized in Table 2. Positional and displacement parameters refined are given in Table 3, selected interatomic distances in Table 4, and coordination-polyhedron characteristics, calculated with the IVTON program (Balić-Žunić & Vicković 1996), in Table 5. Tables listing the observed and calculated structure-factors may be obtained from the Depository of Unpublished Data on the Mineralogical Association of Canada website [document Guettardite CM50_253]. The site labeling and the crystal structure of guettardite are illustrated in Figures 1 and 2, respectively.

Description of the Structure

In the current refinement of the structure, the lattice parameters of the single crystal of guettardite from Barika were determined to be *a* 8.527(4), *b* 7.971(4), *c* 20.102(10) Å, β 101.814(7)°, space group $P2_1/c$. For comparison, lattice parameters of the type guettardite from Madoc, obtained from Weissenberg and precession photographs, were described as *a* 20.0(4), *b* 7.94(3), *c* 8.72(6) Å, β 101.58(50)° (Jambor 1967a). The data for the Tuscany material (precession data refined using X-ray powder-diffraction data) are *a* 20.05(5), *b* 7.95(2), *c* 8.44(2) Å, β 102.77(17)° (Bracci *et al.* 1980). Both Jambor and Bracci *et al.* determined the space group as $P2_1/a$. Thus, no significant differences between the lattice data, obtained by widely different methods, are observed.

The topology of the crystal structure of guettardite corresponds to that of the sartorite subcell, as determined by Iitaka & Nowacki (1961). According to the scheme suggested by Makovicky (1985), the structure

TABLE 3. FINAL COORDINATES AND ANISOTROPIC DISPLACEMENT PARAMETERS (Å^2) OF ATOMS IN GUETTARDITE

ATOM	*x*	*y*	*z*	sof	U_{eq}	U_{11}	U_{22}	U_{33}	U_{23}	U_{13}	U_{12}
Pb1	0.5174(2)	0.0926(2)	0.7975(1)	1	0.036(1)	0.036(1)	0.036(1)	0.034(1)	0.006(1)	0.002(1)	-0.010(1)
Pb2	0.0243(2)	0.0854(2)	0.8027(1)	1	0.050(1)	0.049(1)	0.066(1)	0.039(1)	0.020(1)	0.020(1)	0.028(1)
Sb1	0.9116(2)	0.1951(3)	0.0256(1)	0.98(1)	0.025(1)	0.029(2)	0.018(2)	0.028(2)	-0.001(1)	0.006(1)	0.002(1)
Sb2	0.6597(3)	0.0196(3)	0.6132(1)	0.94(1)	0.028(1)	0.038(2)	0.017(2)	0.027(2)	0.0004(10)	0.004(1)	-0.002(1)
As1	0.3586(4)	0.1708(4)	0.9940(2)	0.98(2)	0.022(1)	0.019(2)	0.016(2)	0.031(2)	0.007(2)	0.001(2)	0.002(2)
As2	0.8067(4)	0.0063(4)	0.3681(2)	1.05(2)	0.023(1)	0.021(2)	0.024(2)	0.023(2)	-0.002(2)	-0.001(1)	0.003(1)
S1	0.1403(10)	0.0094(10)	0.0764(4)	1	0.020(2)	0.022(4)	0.015(5)	0.023(4)	0.009(4)	0.005(3)	-0.007(3)
S2	0.7043(10)	0.0416(10)	0.0840(4)	1	0.024(2)	0.035(5)	0.017(5)	0.023(5)	-0.006(4)	0.013(4)	-0.003(4)
S3	0.5440(10)	0.1933(10)	0.4419(5)	1	0.032(2)	0.035(5)	0.020(5)	0.044(6)	-0.012(4)	0.015(4)	0.002(4)
S4	0.4148(10)	0.1675(10)	0.6574(4)	1	0.019(2)	0.018(4)	0.018(5)	0.022(4)	-0.007(4)	0.004(3)	0.009(4)
S5	0.1506(10)	0.1584(10)	0.4531(5)	1	0.034(2)	0.030(5)	0.015(5)	0.068(7)	-0.016(4)	0.023(5)	0.002(4)
S6	0.2690(10)	0.1414(10)	0.2817(4)	1	0.021(2)	0.025(4)	0.019(5)	0.020(4)	0.006(4)	0.007(4)	0.005(4)
S7	0.9997(10)	0.1658(10)	0.6597(4)	1	0.022(2)	0.029(5)	0.019(5)	0.018(4)	0.012(4)	0.006(4)	0.000(4)
S8	0.7558(10)	0.1549(10)	0.2686(4)	1	0.024(2)	0.027(5)	0.017(5)	0.030(5)	0.001(4)	0.010(4)	0.005(4)

TABLE 4. SELECTED INTERATOMIC DISTANCES (Å) IN GUETTARDITE

Pb1-	S4	2.836(8)	Pb2-	S7	2.912(8)	Sb1-	S1	2.494(8)
	S6	2.968(8)		S8	3.058(8)		S1	2.585(8)
	S8	3.001(8)		S2	3.068(8)		S2	2.617(9)
	S8	3.133(8)		S6	3.103(8)		S7	2.868(8)
	S6	3.244(9)		S1	3.138(9)		S5	2.976(10)
	S3	3.335(9)		S8	3.215(9)		S3	3.360(8)
	S2	3.498(9)		S6	3.265(8)		S5	3.768(9)
	S4	3.524(8)		S7	3.445(8)			
	S1	3.546(7)		S5	3.625(10)			
Sb2-	S6	2.441(8)	As1-	S5	2.254(9)	As2-	S8	2.289(8)
	S3	2.516(9)		S2	2.296(9)		S7	2.301(9)
	S5	2.699(10)		S3	2.335(10)		S4	2.314(8)
	S4	2.702(9)		S1	3.021(9)		S3	3.286(10)
	S7	3.087(8)		S2	3.292(8)		S5	3.307(9)
	S2	3.580(9)		S4	3.469(9)		S5	3.773(10)
	S3	3.654(8)						

TABLE 5. POLYHEDRON CHARACTERISTICS IN GUETTARDITE

Atom	1	2	3	4	5	6	7	8
Pb1	9	3.223	0.014	0.343	0.978	140.195	67.649	1.777
Pb2	9	3.199	0.027	0.171	0.825	137.070	65.229	1.759
Sb1	7	2.979	0.107	0.573	0.897	110.780	37.436	2.897
Sb2	7	2.941	0.094	0.585	0.875	106.530	36.536	3.142
As1	6	2.784	0.096	0.646	0.958	90.419	26.031	2.968
As2	6	2.914	0.115	0.718	0.895	103.634	29.207	2.822
S1	5	3.012	0.223	0.489	0.953	114.473	18.394	1.982
S2	6	3.096	0.107	0.615	0.917	124.251	35.321	1.976
S3	6	3.071	0.102	0.472	0.680	121.308	34.677	1.960
S4	5	2.996	0.104	0.566	0.856	112.601	20.871	1.942
S5	7	3.166	0.113	0.460	0.589	132.873	44.620	1.927
S6	5	3.080	0.227	0.518	0.962	122.406	19.559	1.870
S7	5	2.927	0.045	0.538	0.954	105.042	20.739	1.862
S8	5	3.119	0.357	0.612	0.995	127.100	16.909	1.846

The polyhedron characteristics used were defined in Balić-Žunić & Makovicky (1996) and Makovicky & Balić-Žunić (1998): 1) coordination number, 2) radius r_s in Å of a circumscribed sphere, least-squares fitted to the coordination polyhedron, 3) volume distortion υ = [V(ideal polyhedron) – V(real polyhedron)]/V(ideal polyhedron); the ideal polyhedron has the same number of ligands, 4) "volume-base" eccentricity $ECC_V = 1 - [(r_s - \Delta)/r_s]^3$; Δ is the distance between the center of the sphere and the central atom in the polyhedron, 5) "volume-based" sphericity $SPH_V = 1 - 3\sigma_r r_s$; σ_r is a standard deviation of the radius r_s, 6) volume in Å^3 of the circumscribed sphere, 7) volume in Å^3 of coordination polyhedron, 8) bond-valence sum.

consists of $(30\bar{1})$ slices of modified SnS archetype, joined *via* zig-zag layers of tricapped coordination prisms of Pb (Fig. 2). The slices contain two distinct [100] columns of coordination pyramids occupied by As and Sb; these pyramids can be completed to monocapped trigonal coordination prisms of the metalloid atoms, in which the spaces occupied by lone pairs of electrons are included. The slices are three coordination polyhedra wide if the Pb position flanking the slice is counted as well. It is the lowest homologue (N = 3) of the sartorite homologous series that can exist for a given combination of cations and anions. In both columns of coordination pyramids, arsenic and antimony alternate along [100], forming ribbons with a checker-board distribution of As and Sb.

The structure of guettardite contains six distinct coordination polyhedra of cations. Lead, in Pb1 and Pb2 sites that alternate in each column of lead coordination prisms, forms slightly skewed trigonal coordination prisms completed by three additional caps. Distances in the latter show best the irregularity of lead coordination: the capping Pb–S distances, 2.836 Å and 2.912 Å (for Pb1 and Pb2, respectively), are opposed by the capping Pb–S distances, equal to or much larger than 3.33 Å (Fig. 2, Table 4). The one-sidedness of the Pb1 position is more pronounced than that of Pb2, but Pb2 shows a more pronounced anisotropic displacement around the more symmetric mean position. The S6–S8 distances along [100] are 4.21 and 4.33 Å for Pb1 and

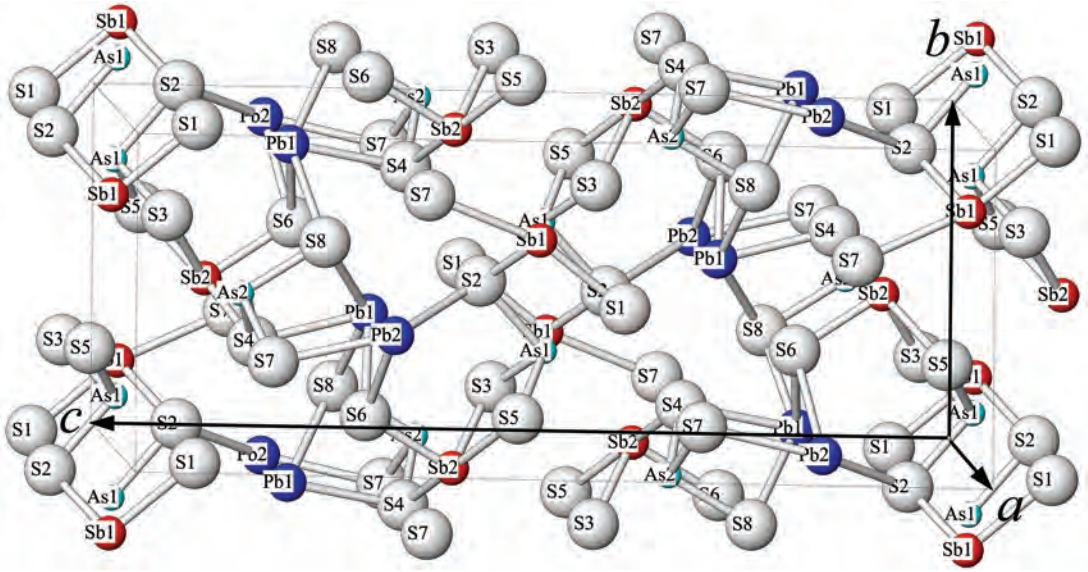

FIG. 1. Site labeling for the crystal structure of guettardite. Oblique projection on (100).

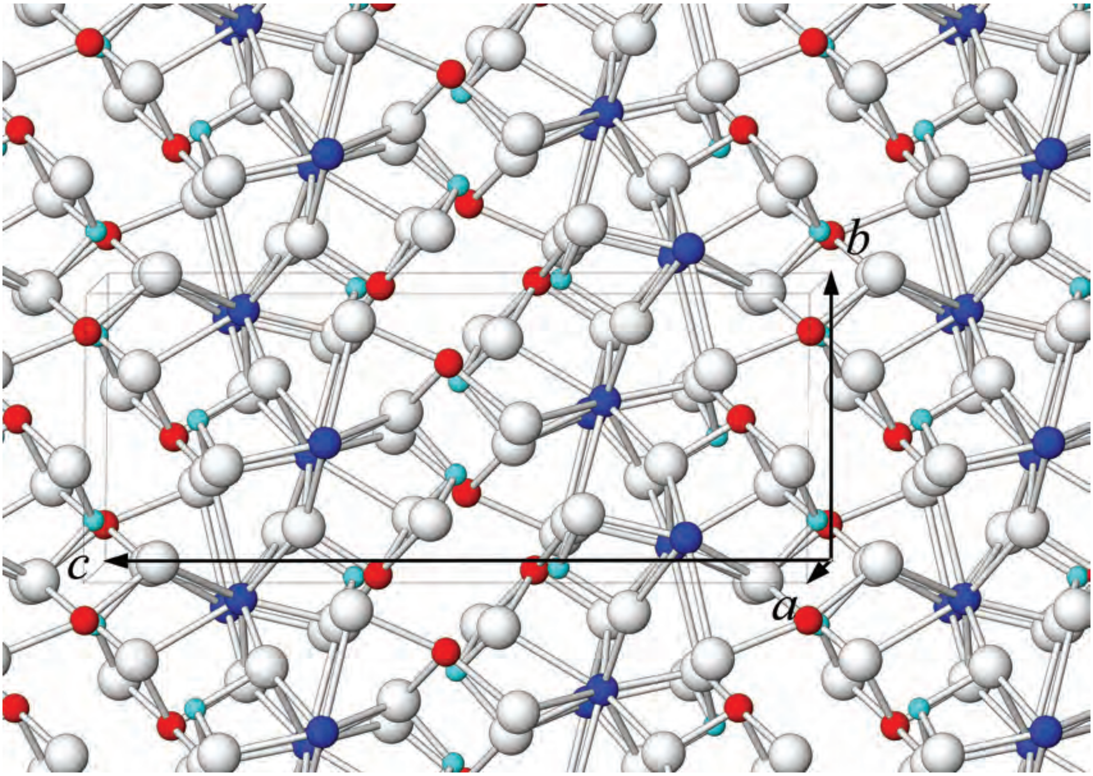

FIG. 2. The crystal structure of guettardite in oblique projection on (100). In order of decreasing size, circles represent S, Pb (blue), Sb (red) and As (green). Only prominent cation–anion distances are indicated.

Pb2, respectively. The S1–S2 distances, however, are 4.79 and 3.76 Å, in the same order. Such a distortion of the coordination prism of Pb2 is connected with the structural details of the Sb–As-containing portions of the structure and concurs with its anisotropic behavior. No distances shorter than typical Pb–S distances in the sartorite homologues (Berlepsch *et al.* 2001a) have been observed.

The coordination polyhedra of arsenic and antimony are well individualized, precluding significant mixing of these two cations at the same sites. The short S–As bonds of As1 and As2 are tightly concentrated about 2.254–2.335 and 2.289–2.314 Å, respectively (Table 4). Only the two longer As–S distances in the base of the coordination pyramid of As2 are symmetrical (3.286–3.307 Å); those of As1 complete an asymmetric trapezoidal coordination, with As–S distances 3.021 and 3.292 Å, respectively (Fig. 3). The configurational background of this difference will be explained further below. Trapezoidally coordinated Sb1, with three short Sb–S bonds between 2.494 and 2.617 Å, has asymmetric long distances, 2.976 and 3.360 Å, respectively. The Sb2 atom exhibits a more complicated bonding scheme: the opposing distances to S4 and S5 in the trapezoidal base are 2.70(3) Å long, whereas the two remaining opposing distances in this base are very different, 2.516 and 3.087 Å, respectively. The shortest Sb – S distance, 2.441 Å, is oriented toward the vertex of the pyramid; for Sb1, this distance is 2.585 Å. In order to verify whether the observed bonding-scheme

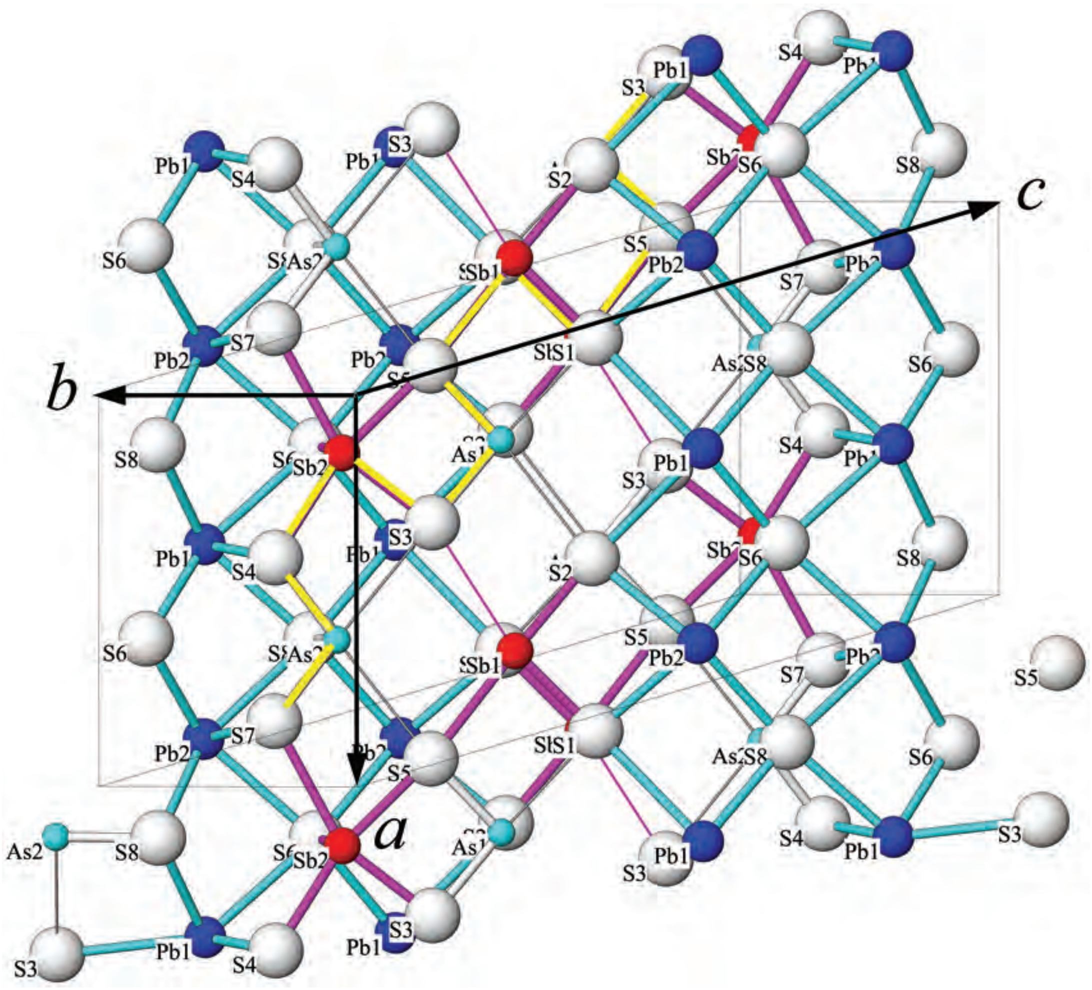

FIG. 3. A tightly bonded double-layer from the crystal structure of guettardite nearly parallel to (012). Coloring of atoms is as in Figure 2. The Pb–S distances, and short Sb–S (red) and As–S (white) distances are indicated by bold lines. One crankshaft chain is accentuated by a yellow outline.

of Sb2 is genuine or a result of two overlapping, statistically occupied Sb positions, the ratios of lengths of the opposing bonds were compared with the ratios dictated by element-specific bond-length hyperbolae (Berlepsch *et al.* 2001a, 2001b, Topa & Makovicky 2010). The parameters of the hyperbola equation $(x - a)(y - a) = c$, where x and y are lengths of two opposing bonds (in Å), and a and c are constants resulting from a fitting procedure to a number of observed coordinations, were calculated by Berlepsch *et al.* (2001a) for the hyperbola of antimony as $a = 2.384$ and $c = 0.0895$. This model dictates a bond length of 2.683 Å for the case $x = y$, close to our S4 – Sb2 – S5 coordination, 2.70(3) Å, confirming that we have a rather rarely occurring Sb (2 + 2 + 2) coordination. A bond-length ratio far from the hyperbola would suggest a split position. The rest of bond lengths of Sb2 and those of Sb1 are disposed along the flanks of the hyperbola.

The separation of As and Sb suggested by the bonding schemes of respective cation sites has been confirmed by a free refinement of their occupancies. The Pb and S sites were fixed to full occupancy, as indicated by previous cycles of refinement. Both Sb1 and As1 refined to practically full occupancy (Table 3), whereas As2 refined to 1.05 and Sb2 to 0.94 atoms per site, suggesting a small degree of As–Sb mixing at the Me2 sites, within two standard deviations in the case of As2. Polyhedron volumes (CN = 7) are in agreement with these conclusions, the volume of Sb2 being slightly smaller and that of As2 somewhat larger than the volumes of pure Sb1 and As1 polyhedra (Table 5). Inspection of anisotropic displacement parameters (Table 3) does not reveal any unusual values. Atom Pb2 has larger displacements than Pb1 but a marginally smaller volume of its polyhedron (Table 5).

The configuration of the SnS-like slices follows to a great degree that outlined for sartorite homologues by Makovicky (1985) and Berlepsch *et al.* (2001a). The SnS-like slices contain tightly bonded double-layers with short, strong Me–S bonds interconnecting their two surfaces. They are separated by more voluminous interspaces into which the lone pairs of electrons of Sb and As are oriented (Fig. 2). In the surfaces of the double layer, a tier with Pb1–As1–Sb2 polyhedra alternates along [100] with a tier with Pb2– Sb1–As2 polyhedra (Fig. 3). The interatomic distances across the core of the lone-electron-pair micelle are considerable (Table 4), except for the distance Sb1–S7, situated in the tight corner of the micelle and equal to 2.868 Å, This distance is opposed by a shorter distance of 2.585 Å to the vertex of the Sb1 pyramid. In general, the two cation–anion distances that span the core space are very different, especially for Sb1 and As1, leading to "lying-down" distorted monocapped trigonal prisms of As and Sb.

The interior of the double layer is structured as well. Figure 3 shows that it contains a series of parallel, imperfectly configured "crankshaft chains" of short Sb–S and As–S bonds, in the sequence As2–Sb2–As1–Sb1–Sb1–As1–Sb2–As2. They run diagonally across a tightly bonded double-layer and are separated from the adjacent crankshaft chains by intervals occupied by long cation–anion distances (Fig. 3). The influence of lone-electron pairs extends thus not only into the interlayer space but also into these inflated gaps in the double layers themselves. In the crankshaft chains, the tightly bonded configuration S1–Sb1–S1–Sb1–S1 is well defined, whereas that of the Sb2–As2 pair appears to fluctuate between the "open" crankshaft-like S4–Sb2–S3–As1–S5 configuration and the "closed" S3–Sb2–S5–As1–S3 configuration, which is a tightly bonded cation pair; the latter displays a short common S3–S5 edge. The two-tier accommodation of lone-electron pairs in guettardite, involving crankshaft chains, is shared with the Pb–As phases of the sartorite homologous series (Makovicky 1985, Berlepsch *et al.* 2001a).

The purely arsenian homeotype of guettardite, sartorite, with a structural formula alternatively simplified to $PbAs_2S_4$ (Iitaka & Nowacki 1961) and expanded to $Pb_8Tl_{1.5}As_{17.5}S_{35}$ (Berlepsch *et al.* 2003), exhibits a complicated superstructure or, perhaps, a series of superstructures (Bannister *et al.* 1939, Berry 1943, Nowacki *et al.* 1961, Pring *et al.* 1993, Pring 2001, Ozawa & Takeuchi 1993, Berlepsch *et al.* 2003). The only superstructure resolved by X-ray diffraction and structure determination is a nine-fold superstructure with the above formula, *a* 9 × 4.19, *b* 7.898, *c* 20.106 Å, β 101.99° (Berlepsch *et al.* 2003). Its double layer contains crankshaft chains in two orientations at 90° to one another, closed-to-open As–As pairs and other split As and As(Tl) positions, even a missing S site. Parts of the Pb column resemble our Pb1–Pb2 configuration, but this configuration gets obliterated in another portion of the column, allowing a nine-fold repetition, not compatible with the trapezoidal pattern observed in guettardite. With its regular trapezoidal pattern in the Sb–As portions of the structure, and the solution of mutual fit problems between the metalloid-containing portions and the Pb-containing portions of the structure by incorporation of Sb in a checkerboard pattern, guettardite preserves a simple 2 × 4.26 Å periodicity. In this, it is similar to the N = 4 homologues of sartorite (which have certain amounts of Pb and Ag forming a regular pattern of substitution in the metalloid-based portions of their structures), but it is different from the complicated solution found in sartorite itself.

The crystal structure of another homeotype, synthetic $BaSb_2S_4$ (Cordier *et al.* 1984), follows the pattern of sartorite homologues: a zig-zag layer of nine-coordinated Ba alternating with SnS-like slabs constituted by coordination polyhedra of antimony. The more tightly bonded double layers of the SnS-like motif are further subdivided into diagonally running, more tightly bonded Sb–S chains separated by interspaces with longer Sb–S distances, of the order of 3.3–3.6 Å (Fig. 4). Those distances in the chains that oppose

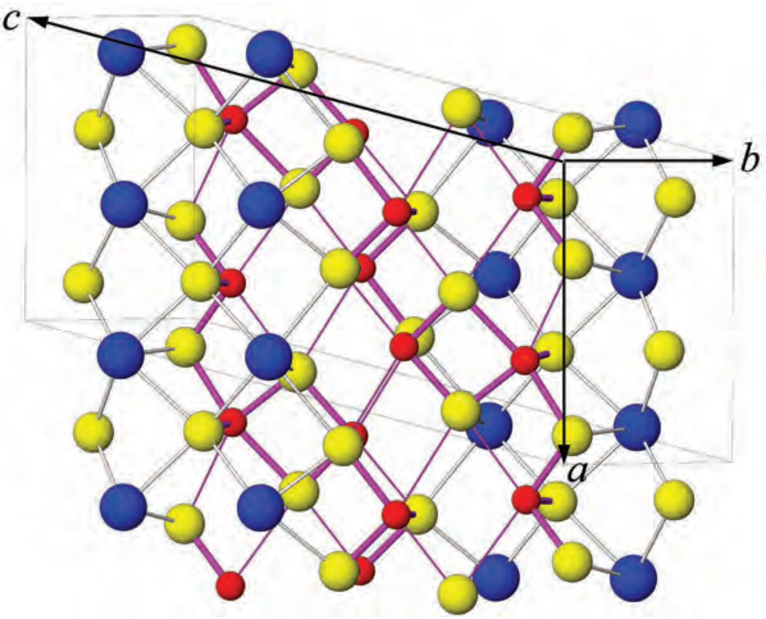

FIG. 4. A double layer (~012) from the crystal structure of $BaSb_2S_4$ (Cordier *et al.* 1984). Barium is blue, Sb is red; short Sb–S distances (bold, red) form crankshaft chains.

these longer distances are only 2.4–2.6 Å. The Sb3 atom has a quasi-symmetrical coordination of 2.6–2.9 Å bonds opposing one another. The SbS_5 pyramids have pronounced trapezoidal bases, deformed somewhat by an alternation of chains and larger interspaces reserved for the lone pairs of electrons. The tightly bonded crankshaft chains are anchored on mirror-symmetrical Sb1 polyhedra. Thus, $BaSb_2S_4$ shares many of the features that we have seen in guettardite. The alternation of trapezoids and diagonal chains along the [100] direction leads to the 2 × 4.49 Å periodicity. The lattice parameters *a* 8.985, *b* 8.203, *c* 20.602 Å, β 101.36° and the space group $P2_1/c$ confirm its remarkable similarity to guettardite.

The β angle of guettardite is determined by the orientation of the crankshaft chains in the sequence of $(001)_{\text{gtd}}$ SnS-like slices following one another in the general [001]* direction. They obey a **c**-glide plane parallel to (010), *i.e.*, for both sets of the alternating slices produced by the glide operation, these chains point in the $[20\bar{1}]$ direction if projected upon (010) as illustrated in Figure 5. From the starting As2 to the As2 atom at the opposite end of the crankshaft chain, the chain "descends" by 3.5 × 4.2 Å; in the gap between two adjacent chains of the same SnS-based slice, the opposing polyhedra of As2 are only 1.5 × 4.2 Å apart if displacements along the [100] direction are considered.

Across the zig-zag Pb "boundary", As1 polyhedra from two adjacent Sb–As-based slabs form a zig-zag arrangement; the [100] components of the shifts between such neighbors are 4.2 Å. The same holds for As2. The mutual displacement of the centers of chains in neighboring SnS-like slices is only 0.5 × 4.2 Å along [100]. This results in a "monoclinicity" of the unit cell: Δ*a* is approximately one subcell period (~4.1 Å) across every *d*(001) interval. The 2_1 operations relating adjacent Sb–As-based slabs are situated in the layer of Pb coordination prisms.

With respect to the possible stacking variants of Sb–As–S chains, we divide the structure into two types of alternating OD layers. These slices are parallel to $(001)_{\text{gtd}}$. The first type of OD layers consists of tricapped trigonal coordination prisms of Pb1 and Pb2, to which the As2 polyhedra are added in Figure 6 in order to stress the regular alternation of these "anchoring" elements on the surfaces of the layers just defined. Study of Figure 6 shows that with or without As2 polyhedra, the layer-group symmetry of this layer is $Pm2_1(n)$, where the bracketed position denotes the glide plane situated in the median plane of the OD layer. The mirror planes are situated halfway between S3 and S5, on the level of As2 and halfway between As2.

The alternating OD layers (the second type) contain the coordination polyhedra of As1, Sb1 and Sb2. All sulfur atoms are shared with the surfaces of the previous layer, and As2 has been retained as a part of this layer in Figure 7 in order to illustrate their relationship to the first type of layers. The symmetry of the second type of layer is [or $P11(\bar{1})$ in the tables of Dornberger-Schiff & Fichtner (1972)], but its surfaces, especially the configuration of S1, S2, S3 and S5 (Fig. 7), mimic the mirror symmetry indicated for the lead-rich OD layers. Therefore, there is no crystal-chemical difference between the accommodation of the second layer onto the surface of the first layer in the way observed in the current structure, and a mirror-reflected accommodation in which the chains run at about right angle to the original orientation, here depicted. Each chain is anchored on the coordination pyramid of As2 which, by the virtue of its mirror symmetry, accepts their attachment on either side.

As a result of this mirror-reflected accommodation, the disposition of As–Sb-based OD layers of the second type, surrounding the same central Pb-based OD layer of the first kind, will obey the (001) diagonal glide plane, and a 2_1 axis in the **c** direction normal to the layer (a space group $P2_1/n$). This results in a monoclinic unit-cell with γ very close to 90° because of the constraints imposed by the symmetry and configuration of the first type of layer (see the layer group), a unique **c** direction and the *a, b* and *c* parameters corresponding to the *a, b* and *d* (001) parameters of guettardite. And this corresponds to the results obtained for twinnite by Jambor (1967a) if the different crystallographic orientation proposed by him is taken into account. He mentioned only very weak violations of the extinction rules dictated by the symmetry just derived, and he assumed an orthorhombic "pseudocell" and a space group *Pnmn* for which, however, he did not have much evidence. Jambor suggested that twinnite is polysynthetically twinned on (001) (our notation), which disagrees with the X-ray crystallography observed by him and our derivations.

The crystal structure of the $P2_1/n$ polymorph of Ba–Sb chalcogenide $BaSb_2Se_4$ (Cordier & Schäfer 1979) corresponds closely to our model for twinnite. The unit-cell parameters of this compound, *a* 9.237, *b* 20.76, *c* 8.551 Å, β 91.2°, are close to those given for twinnite by Jambor (1967a): *c* 8.60(2), *a* 19.6(2), *b* 7.99(5) Å, all angles equal to 90° (original orientations used). The differences in radius between Sb and (As,Sb), as well as Ba and Pb, and Se and S, must all be taken into account in this comparison. We interpret Jambor's systematic extinctions as $P2_1/n11$, *i.e.*, he used a setting with a unique **a** axis.

Just as $BaSb_2S_4$, the structure of $BaSb_2Se_4$ is a homeotype of sartorite with a 4.60 Å × 2 periodicity.

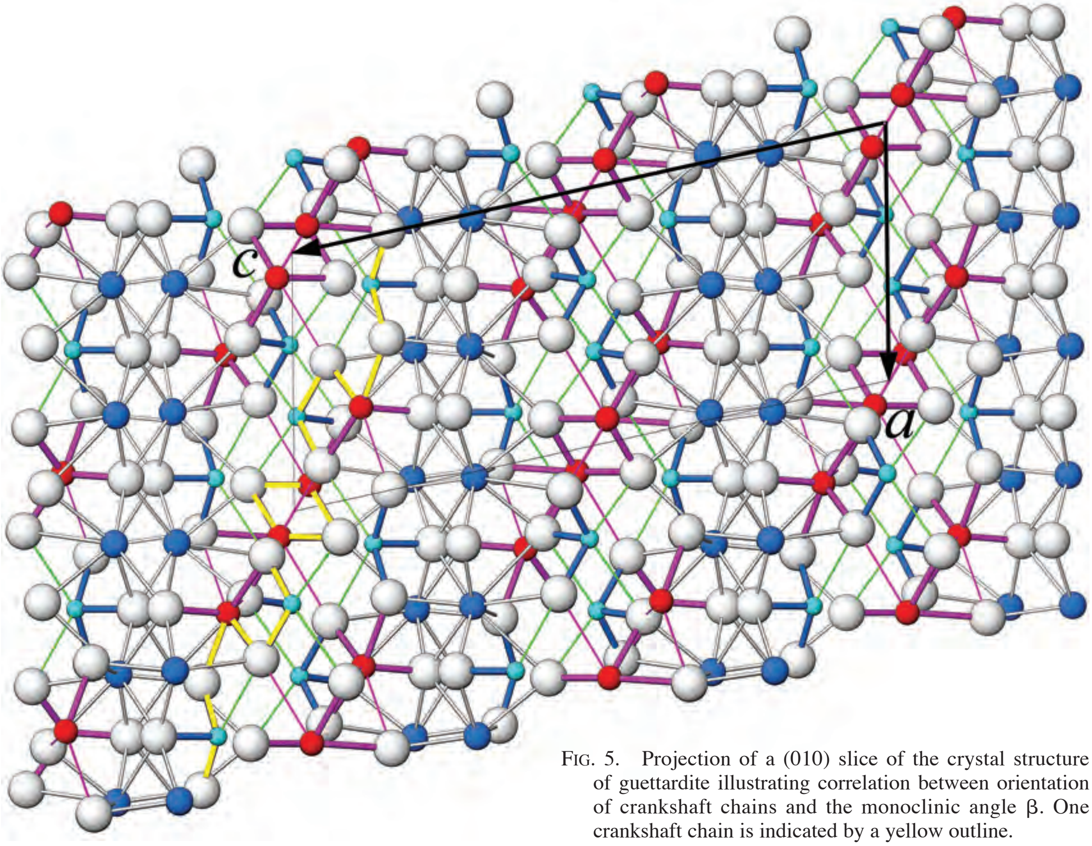

FIG. 5. Projection of a (010) slice of the crystal structure of guettardite illustrating correlation between orientation of crankshaft chains and the monoclinic angle β. One crankshaft chain is indicated by a yellow outline.

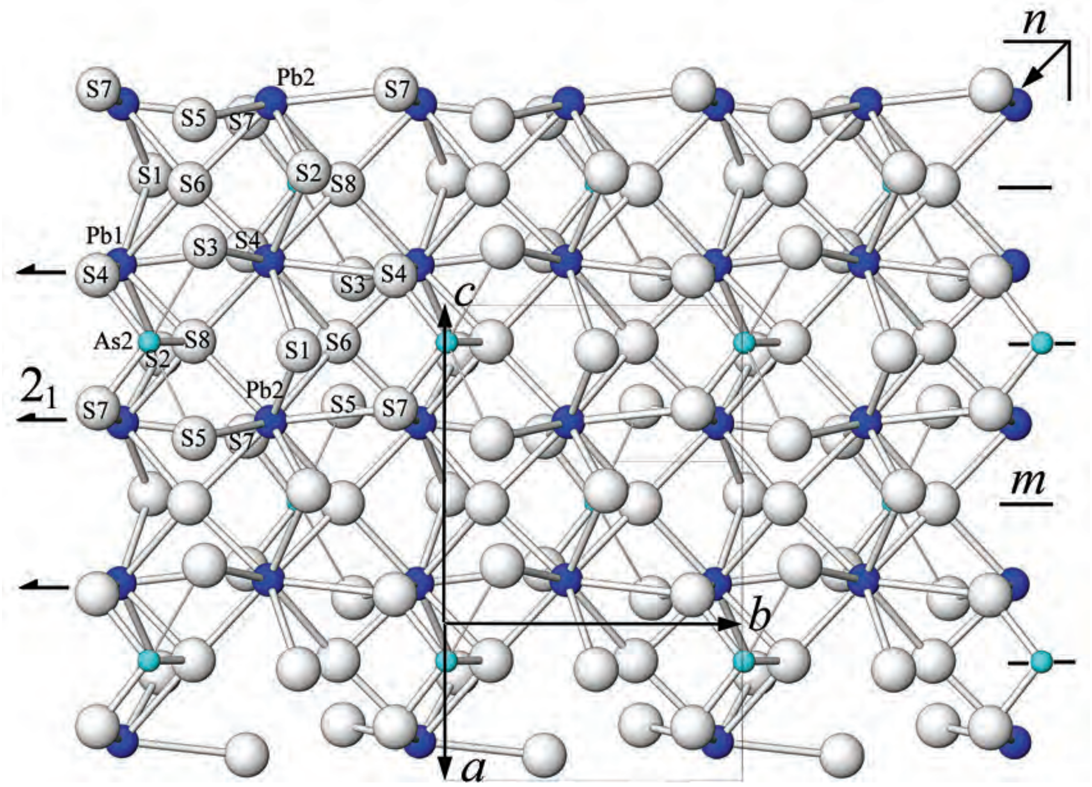

FIG. 6. The first type of OD layer (the Pb-based layer OD1) participating in the OD structure of guettardite. Slightly idealized symmetry of the layer is $Pm2_1(n)$. The diagonal glide plane is parallel to the layer. The Pb–S distances and short As–S distances are shown as bold lines, and the long As–S distances, as thin lines. The Pb atoms are shown in blue, and As atoms, in turquoise.

The Sb-containing layers of $BaSb_2Se_4$ are based on the SnS archetype, with the tightly bonded double layers separated by long Sb–Se distances, of the order of 3.30–3.65 Å. The exception is bonding of Sb4, which has a near-symmetrical coordination with the distance 2.85 Å opposed by 2.80 Å; the latter distance spans the interspace used by the lone pairs of electrons belonging to other Sb atoms. The more tightly bonded double layer again contains diagonally arranged crankshaft chains of short bonds (2.56–2.67 Å) separated by intervals with Sb–Se distances equal to 3.31–3.72 Å. The $SbSe_5$ coordination pyramids have trapezoidal bases, similar to $BaSb_2S_4$. Where required, the latter long distances make the trapezoidal bases asymmetric because inside the crankshaft arrangement, the longest distances are only 2.92–3.12 Å. The exception is Sb1 adjacent to the large coordination polyhedron of barium.

The arrangement of crankshaft chains in the adjacent SnS-like layers obeys the *n* glide plane in the median plane of the Ba-based interlayer, exactly as predicted by us for twinnite. The symmetrical Sb1 pyramids are the "chain-anchoring elements", with a function analogous to As2 in guettardite. Thus, although different in chemical composition, $BaSb_2S_4$ and $BaSb_2Se_4$ are polytypes from a configurational point of view and model substances for the guettardite–twinnite pair.

CONCLUSIONS

Although new investigations on twinnite are still pending, we propose that $PbAsSbS_4$ is an OD (order–disorder) structure in a sense of Dornberger-Schiff (1956), Ďurovič (1997) and Merlino (1997), with two types of OD layers, $Pm2_1(n)$ and $P\overline{1}$, respectively, in regular alternation. In this scheme, guettardite is a $P2_1/c$ polytype, whereas "twinnite" is a $P2_1/n$ polytype with a different stacking principle and orientation of symmetry elements. Stacking faults will generally be inevitable in both structures and will result in the twinning observed. Whether differences in the Sb:As ratio of the original specimens are the reason for the two stacking modes observed cannot be established at present because, on

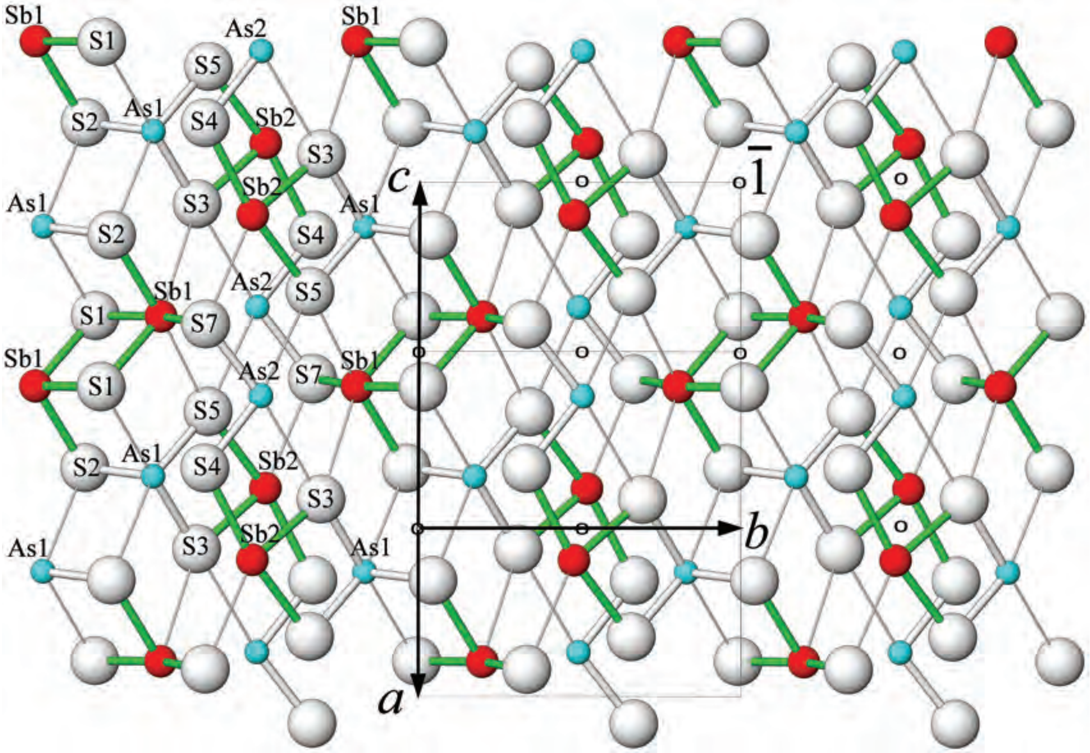

FIG. 7. The As–Sb-based OD2 layer from the OD structure of guettardite. A portion of the inversion centers of the layer group $P\bar{1}$ are indicated by small circles. Short As–S distances (white) and Sb–S distances (green) are indicated by bold lines, and the remaining distances, by thin lines. The Sb atoms are shown in red, and As atoms, in turquoise.

the one hand, the early electron-microprobe data carry considerable systematic errors, and on the other hand, only a limited amount of the material is available for research. The guettardite–twinnite pair appears to be paralleled by homeotypes constituting the $BaSb_2S_4$ and $BaSb_2Se_4$ pair.

ACKNOWLEDGEMENTS

We gratefully acknowledge the financial support the Research Council for the Nature and Universe, Denmark (grant no. 272–08–0227) and of the Christian Doppler Foundation (Austria). The manuscript benefitted from comments of Dr. Daniela Pinto and an unknown referee, and from the editorial care of Dr. Tonči Balić-Žunić and Prof. Robert F. Martin.

REFERENCES

BALIĆ-ŽUNIĆ, T. & MAKOVICKY, E. (1996): Determination of the centroid or 'the best centre' of a coordination polyhedron. *Acta Crystallogr.* **B52**, 78-81.

BALIĆ-ŽUNIĆ, T. & VICKOVIĆ, I. (1996): IVTON – program for the calculation of geometrical aspects of crystal structures and some crystal chemical applications. *J. Appl. Crystallogr.* **29**, 305-306.

BANNISTER, F.A., PABST, A. & VAUX, G. (1939): The crystallography of sartorite. *Mineral. Mag.* **25**, 264-270.

BERLEPSCH, P., ARMBRUSTER, T., MAKOVICKY, E. & TOPA, D. (2003): Another step toward understanding the true nature of sartorite: determination and refinement of a ninefold superstructure. *Am. Mineral.* **88**, 450-461.

BERLEPSCH, P., MAKOVICKY, E. & BALIĆ-ŽUNIĆ, T. (2001a): Crystal chemistry of sartorite homologues and related sulfosalts. *Neues Jahrb. Mineral., Abh.* **176**, 45-66.

BERLEPSCH, P., MAKOVICKY, E. & BALIĆ-ŽUNIĆ, T. (2001b): Crystal chemistry of meneghinite homologues and related sulfosalts. *Neues Jahrb. Mineral., Abh.* **176**, 115-135.

BERRY, L.G. (1943): New data on lead sulpharsenides from Binnental, Switzerland. *Am. Mineral.* **38**, 330.

BRACCI, G., DALENA, D., ORLANDI, P., DUCHI, G. & VEZZALINI, G. (1980): Guettardite from Tuscany, Italy: a second occurrence. *Can. Mineral.* **18**, 13-15.

BRUKER AXS (1997): *XPREP, Version 5.1*. Bruker AXS, Inc., Madison,Wisconsin 53719, USA.

BRUKER AXS (1998a): *SMART, Version 5.0*. Bruker AXS, Inc., Madison, Wisconsin 53719, USA.

BRUKER AXS (1998b): *SAINT, Version 5.0*. Bruker AXS, Inc., Madison,Wisconsin 53719, USA.

CIOBANU, C.L., COOK, N.J., CAPRARU, N., DAMINA, G. & CRISTEA, P. (2005): Mineral assemblages from the vein salband at Săcărimb, Golden Quadrilateral, Romania. I. Sulphides and sulphosalts (Au–Ag–Te–Se deposits, IGCP Project 486). *Bulgarian Academy of Sciences, Geochemistry, Mineralogy and Petrology* (*Sofia*) **43**, 47-55.

CORDIER, G. & SCHÄFER, H. (1979): Preparation and crystal-structure of $BaSb_2Se_4$. *Z. Naturforschung* **B34**(8), 1053-1056.

CORDIER, G., SCHWIDETZKY, C. & SCHÄFER, H. (1984): New SbS_2 strings in the $BaSb_2S_4$ structure. *J. Solid State Chem.* **54**, 84-88.

DORNBERGER-SCHIFF, K. (1956): On the order–disorder structures (OD-structures). *Acta Crystallogr.* **9**, 593-601.

DORNBERGER-SCHIFF, K. (1964): Grundzüge einer Theorie von OD-Strukturen aus Schichten, *Abhandlungen der Deutschen Akademie der Wissenschaften zu Berlin, Klasse für Chemie, Geologie und Biologie* **3**, 1-107.

DORNBERGER-SCHIFF, K. (1966): *Lehrgang über OD-Strukturen*. Akademie-Verlag, Berlin, Germany.

DORNBERGER-SCHIFF, K. & FICHTNER, K. (1972): On the symmetry of OD structures consisting of equivalent layers. *Kristall und Technik* **7**, 1035-1056.

ĎUROVIČ, S. (1997): Fundamentals of the OD theory. *In* Modular Aspects of Minerals (S. Merlino, ed.). *Eur. Mineral. Union, Notes in Mineralogy* **1**, 3-28.

FERRARIS, G., MAKOVICKY, E. & MERLINO, S. (2008): *Crystallography of Modular Materials*. Oxford University Press, Oxford, U.K.

IITAKA, Y. & NOWACKI, W. (1961): A refinement of the pseudo crystal structure of scleroclase $PbAs_2S_4$. *Acta Crystallogr.* **14**, 1291-1292.

JAMBOR, J.L. (1967a): New lead sulfantimonides from Madoc, Ontario. 1. *Can. Mineral.* **9**, 7-24.

JAMBOR, J.L. (1967b): New lead sulfantimonides from Madoc, Ontario. 2. Mineral descriptions. *Can. Mineral.* **9**, 191-213.

JAMBOR, J.L. (1968): New lead sulfantimonides from Madoc, Ontario. 3. Syntheses, paragenesis, origin. *Can. Mineral.* **10**, 505-521.

JAMBOR, J.L., LAFLAMME, J.H.G. & WALKER, D.A. (1982): A re-examination of the Madoc sulfosalts. *Mineral. Rec.* **13**, 93-100.

MAKOVICKY, E. (1985): The building principles and classification of sulphosalts based on the SnS archetype. *Fortschr. Mineral.* **63**, 45-89.

MAKOVICKY, E. & BALIĆ-ŽUNIĆ, T. (1998): New measure of distortion for coordination polyhedra. *Acta Crystallogr.* **B54**, 766-773.

MANTIENNE, J. (1974): *La minéralisation metallifère de Jas-Roux* (*Hautes-Alpes*). Thèse de Doctorat, Université de Paris VI, Paris, France.

MERLINO, S. (1997): OD approach in minerals: examples and applications. *In* Modular Aspects of Minerals (S. Merlino, ed.). *Eur. Mineral. Union, Notes in Mineralogy* **1**, 29-54.

MOËLO, Y., MAKOVICKY, E., MOZGOVA, N.N., JAMBOR, J.L., COOK, N., PRING, A., PAAR, W., NICKEL, E.H., GRAESER, S., KARUP-MØLLER, S., BALIĆ-ŽUNIĆ, T., MUMME, W.G., VURRO, F., TOPA, D., BINDI, L., BENTE, K. & SHIMIZU, M. (2008): Sulfosalt systematics: a review. Report of the Sulfosalt sub-committee of the IMA Commission on Ore Mineralogy. *Eur. J. Mineral.* **20**, 7-46.

NOWACKI, W., IITAKA, Y., BÜRKI, H. & KUNZ, V. (1961): Structural investigations on sulfosalts from the Lengenbach, Binn Valley (Ct. Wallis) 2. *Schweiz. Mineral. Petrogr. Mitt.* **41**, 103-116.

OZAWA, T. & TAKÉUCHI, Y. (1993): X-ray and electron diffraction study of sartorite – a periodic antiphase boundary structure and polymorphism. *Mineral. J.* **16**, 358-370.

PAAR, W.H., PRING, A., MOËLO, Y., STANLEY, C.J., PUTZ, H., TOPA, D., ROBERTS, A.C. & BRAITHWAITE, R.S.W. (2009): Daliranite, $PbHgAs_2S_6$, a new sulphosalt from the Zarshouran Au–As deposit, Takab region, Iran. *Mineral. Mag.* **73**, 871-881.

PRING, A. (2001): The crystal chemistry of the sartorite group minerals from Lengenbach, Binntal, Switzerland – a HRTEM study. *Schweiz. Mineral. Petrogr. Mitt.* **81**, 69-87.

PRING, A., WILLIAMS, T. & WITHERS, R. (1993): Structural modulation in sartorite: an electron microscope study. *Am. Mineral.* **78**, 619-626.

SHELDRICK, G.M. (1997a): SHELXS–97. *A Computer Program for Crystal Structure Determination*. University of Göttingen, Göttingen, Germany.

SHELDRICK, G.M. (1997b): SHELXL–97. *A Computer Program for Crystal Structure Refinement*. University of Göttingen, Göttingen, Germany.

TOPA, D. & MAKOVICKY, E. (2010): The crystal chemistry of cosalite based on new electron-microprobe data and single-crystal determinations of the structure. *Can. Mineral.* **48**, 1081-1107.

Received March 10, 2011, revised manuscript accepted March 5, 2012.

APPENDIX: OD STRUCTURES COMPOSED OF MORE THAN ONE KIND OF OD LAYER

The basic elements of OD theory [Dornberger-Schiff (1964); a simple presentation may be found in Ďurovič (1997) and Merlino (1997), and a recent account is given in Ferraris *et al*. (2008)] describe structures built with one type of OD layer. The OD theory has been extended to structures with two or more kinds of OD layers by Dornberger-Schiff (1966) on the basis of the same principle, namely the geometrical equivalence of pairs of adjacent layers, and making use of the same concepts introduced to deal with OD structures consisting of equivalent layers: delineation of OD layers; definition of "λ partial operations of symmetry" (λPOs), *i.e*., finding the group of symmetry operations for each of the distinct OD layers (this group corresponds to one of the 80 layer groups of symmetry); definition of geometric relationships between the adjacent layers; in some cases, definition of "σ partial operations of symmetry" relating adjacent layers where they are of the same kind (as in some phyllosilicates); definition of structures with maximum degree of order (with simplest layer-sequences; these are the two polytypes defined above). The partial character of both sets of operations means that they are not necessarily valid for the whole structure. It seems proper to recall that OD layers have, in general, a purely geometrical meaning and are not always identical with crystal-chemically defined slabs; moreover, as in the present case, they are not necessarily neatly separated, but share common anions with adjacent layers on both sides.

The OD structures with two or more distinct layers may be divided in four categories on the basis of the number of planes containing λ–ρ operations and planes with σ–ρ operations (ρ operations reverse the layer with respect to the direction of the layer stacking, in contrast to so-called τ-operations, which do not reverse the layer). Both types of OD layer in guettardite are nonpolar, presenting the "reversing" λ–ρ POs, which places the guettardite structure in category IV, characterized by 2 λ–ρ planes, one at each OD layer, and 0 σ–ρ planes.

```
data_guettardite

_audit_creation_method            SHELXL-97
_chemical_name_systematic
;
 ?
;
_chemical_name_common             ?
_chemical_melting_point           ?
_chemical_formula_moiety          ?
_chemical_formula_sum
 'As Pb S4 Sb'
_chemical_formula_weight          532.10

loop_
 _atom_type_symbol
 _atom_type_description
 _atom_type_scat_dispersion_real
 _atom_type_scat_dispersion_imag
 _atom_type_scat_source
 'S'  'S'   0.1246   0.1234
 'International Tables Vol C Tables 4.2.6.8 and 6.1.1.4'
 'As'  'As'   0.0499   2.0058
 'International Tables Vol C Tables 4.2.6.8 and 6.1.1.4'
 'Sb'  'Sb'  -0.5866   1.5461
 'International Tables Vol C Tables 4.2.6.8 and 6.1.1.4'
 'Pb'  'Pb'  -3.3944  10.1111
 'International Tables Vol C Tables 4.2.6.8 and 6.1.1.4'

_symmetry_cell_setting           'Monoclinic'
_symmetry_space_group_name_H-M   'P2(1)/c  '

loop_
 _symmetry_equiv_pos_as_xyz
 'x, y, z'
 '-x, y+1/2, -z+1/2'
 '-x, -y, -z'
 'x, -y-1/2, z-1/2'

_cell_length_a                    8.527(4)
_cell_length_b                    7.971(4)
_cell_length_c                    20.102(10)
_cell_angle_alpha                 90.00
_cell_angle_beta                  101.814(7)
_cell_angle_gamma                 90.00
_cell_volume                      1337.3(11)
_cell_formula_units_Z             8
_cell_measurement_temperature     300(2)
_cell_measurement_reflns_used     ?
_cell_measurement_theta_min       ?
_cell_measurement_theta_max       ?

_exptl_crystal_description        ?
_exptl_crystal_colour             ?
```

```
_exptl_crystal_size_max           ?
_exptl_crystal_size_mid           ?
_exptl_crystal_size_min           ?
_exptl_crystal_density_meas       ?
_exptl_crystal_density_diffrn     5.286
_exptl_crystal_density_method     'not measured'
_exptl_crystal_F_000              1840
_exptl_absorpt_coefficient_mu     35.215
_exptl_absorpt_correction_type    ?
_exptl_absorpt_correction_T_min   ?
_exptl_absorpt_correction_T_max   ?
_exptl_absorpt_process_details    ?

_exptl_special_details
;
 ?
;

_diffrn_ambient_temperature       300(2)
_diffrn_radiation_wavelength      0.71073
_diffrn_radiation_type            MoK\a
_diffrn_radiation_source          'fine-focus sealed tube'
_diffrn_radiation_monochromator   graphite
_diffrn_measurement_device_type   ?
_diffrn_measurement_method        ?
_diffrn_detector_area_resol_mean  ?
_diffrn_standards_number          ?
_diffrn_standards_interval_count  ?
_diffrn_standards_interval_time   ?
_diffrn_standards_decay_%         ?
_diffrn_reflns_number             5845
_diffrn_reflns_av_R_equivalents   0.0749
_diffrn_reflns_av_sigmaI/netI     0.0446
_diffrn_reflns_limit_h_min        -8
_diffrn_reflns_limit_h_max        8
_diffrn_reflns_limit_k_min        -7
_diffrn_reflns_limit_k_max        8
_diffrn_reflns_limit_l_min        -20
_diffrn_reflns_limit_l_max        20
_diffrn_reflns_theta_min          2.07
_diffrn_reflns_theta_max          20.91
_reflns_number_total              1264
_reflns_number_gt                 1101
_reflns_threshold_expression      >2sigma(I)

_computing_data_collection        ?
_computing_cell_refinement        ?
_computing_data_reduction         ?
_computing_structure_solution     'SHELXS-97 (Sheldrick, 1990)'
_computing_structure_refinement   'SHELXL-97 (Sheldrick, 1997)'
_computing_molecular_graphics     ?
_computing_publication_material   ?

_refine_special_details
;
```

```
 Refinement of F^2^ against ALL reflections.  The weighted R-factor wR and
 goodness of fit S are based on F^2^, conventional R-factors R are based
 on F, with F set to zero for negative F^2^. The threshold expression of
 F^2^ > 2sigma(F^2^) is used only for calculating R-factors(gt) etc. and is
 not relevant to the choice of reflections for refinement.  R-factors based
 on F^2^ are statistically about twice as large as those based on F, and R-
 factors based on ALL data will be even larger.
;

_refine_ls_structure_factor_coef  Fsqd
_refine_ls_matrix_type            full
_refine_ls_weighting_scheme       calc
_refine_ls_weighting_details
 'calc w=1/[\s^2^(Fo^2^)+(0.0364P)^2^+150.9698P] where P=(Fo^2^+2Fc^2^)/3'
_atom_sites_solution_primary      direct
_atom_sites_solution_secondary    difmap
_atom_sites_solution_hydrogens    geom
_refine_ls_hydrogen_treatment     mixed
_refine_ls_extinction_method      SHELXL
_refine_ls_extinction_coef        0.00002(7)
_refine_ls_extinction_expression
 'Fc^*^=kFc[1+0.001xFc^2^\l^3^/sin(2\q)]^-1/4^'
_refine_ls_number_reflns          1264
_refine_ls_number_parameters      132
_refine_ls_number_restraints      0
_refine_ls_R_factor_all           0.0666
_refine_ls_R_factor_gt            0.0583
_refine_ls_wR_factor_ref          0.1212
_refine_ls_wR_factor_gt           0.1173
_refine_ls_goodness_of_fit_ref    1.090
_refine_ls_restrained_S_all       1.090
_refine_ls_shift/su_max           0.000
_refine_ls_shift/su_mean          0.000

loop_
 _atom_site_label
 _atom_site_type_symbol
 _atom_site_fract_x
 _atom_site_fract_y
 _atom_site_fract_z
 _atom_site_U_iso_or_equiv
 _atom_site_adp_type
 _atom_site_occupancy
 _atom_site_symmetry_multiplicity
 _atom_site_calc_flag
 _atom_site_refinement_flags
 _atom_site_disorder_assembly
 _atom_site_disorder_group
Pb1 Pb 0.51738(17) 0.09255(19) 0.79750(7) 0.0363(6) Uani 1 1 d . . .
Pb2 Pb 0.02426(19) 0.0854(2) 0.80266(8) 0.0496(6) Uani 1 1 d . . .
Sb1 Sb 0.9116(3) 0.1951(3) 0.02558(11) 0.0248(10) Uani 0.977(10) 1 d P . .
Sb2 Sb 0.6597(3) 0.0196(3) 0.61316(11) 0.0276(11) Uani 0.943(11) 1 d P . .
As1 As 0.3586(4) 0.1708(4) 0.99402(17) 0.0224(14) Uani 0.984(15) 1 d P . .
As2 As 0.8067(4) 0.0063(4) 0.36812(15) 0.0234(14) Uani 1.049(15) 1 d P . .
S1 S 0.1403(9) 0.0094(10) 0.0764(4) 0.0201(19) Uani 1 1 d . . .
```

```
S2 S 0.7043(10) 0.0416(10) 0.0840(4) 0.024(2) Uani 1 1 d . . .
S3 S 0.5440(10) 0.1932(11) 0.4419(4) 0.032(2) Uani 1 1 d . . .
S4 S 0.4148(9) 0.1675(10) 0.6574(4) 0.0193(18) Uani 1 1 d . . .
S5 S 0.1506(10) 0.1584(11) 0.4531(5) 0.036(2) Uani 1 1 d . . .
S6 S 0.2689(9) 0.1414(10) 0.2817(4) 0.0207(19) Uani 1 1 d . . .
S7 S 0.9997(9) 0.1658(10) 0.6596(4) 0.0220(19) Uani 1 1 d . . .
S8 S 0.7558(9) 0.1549(10) 0.2686(4) 0.024(2) Uani 1 1 d . . .

loop_
 _atom_site_aniso_label
 _atom_site_aniso_U_11
 _atom_site_aniso_U_22
 _atom_site_aniso_U_33
 _atom_site_aniso_U_23
 _atom_site_aniso_U_13
 _atom_site_aniso_U_12
Pb1 0.0364(9) 0.0364(10) 0.0336(9) 0.0056(7) 0.0015(6) -0.0097(7)
Pb2 0.0486(11) 0.0658(12) 0.0390(10) 0.0202(8) 0.0200(7) 0.0279(9)
Sb1 0.0290(15) 0.0175(15) 0.0281(15) -0.0009(10) 0.0059(10) 0.0015(11)
Sb2 0.0383(18) 0.0166(16) 0.0267(16) 0.0004(11) 0.0040(11) -0.0024(11)
As1 0.019(2) 0.016(2) 0.031(2) 0.0068(15) 0.0009(14) 0.0017(15)
As2 0.021(2) 0.024(2) 0.023(2) -0.0016(15) -0.0005(13) 0.0028(14)
S1 0.022(4) 0.015(4) 0.023(4) 0.009(4) 0.004(3) -0.007(3)
S2 0.035(5) 0.017(5) 0.023(4) -0.006(4) 0.013(4) -0.003(4)
S3 0.034(5) 0.020(5) 0.044(5) -0.012(4) 0.015(4) 0.002(4)
S4 0.018(4) 0.018(4) 0.022(4) -0.007(4) 0.004(3) 0.009(4)
S5 0.030(5) 0.015(5) 0.068(7) -0.016(4) 0.023(5) 0.002(4)
S6 0.025(4) 0.019(5) 0.019(4) -0.006(3) 0.006(3) 0.005(4)
S7 0.029(5) 0.019(5) 0.018(4) 0.012(4) 0.006(4) 0.000(4)
S8 0.027(5) 0.017(5) 0.030(5) 0.001(4) 0.010(4) 0.005(4)

_geom_special_details
;
 All esds (except the esd in the dihedral angle between two l.s. planes)
 are estimated using the full covariance matrix.  The cell esds are taken
 into account individually in the estimation of esds in distances, angles
 and torsion angles; correlations between esds in cell parameters are only
 used when they are defined by crystal symmetry.  An approximate (isotropic)
 treatment of cell esds is used for estimating esds involving l.s. planes.
;

loop_
 _geom_bond_atom_site_label_1
 _geom_bond_atom_site_label_2
 _geom_bond_distance
 _geom_bond_site_symmetry_2
 _geom_bond_publ_flag
Pb1 S4 2.837(8) . ?
Pb1 S6 2.968(8) 4_566 ?
Pb1 S8 3.001(8) 4_566 ?
Pb2 S7 2.911(7) 1_455 ?
Pb2 S8 3.058(8) 4_466 ?
Pb2 S2 3.068(8) 3_656 ?
Pb2 S6 3.104(8) 4_566 ?
Sb1 S1 2.494(8) 1_655 ?
```

```
Sb1 S1 2.586(8) 3_655 ?
Sb1 S2 2.618(9) . ?
Sb1 S7 2.868(8) 4_565 ?
Sb2 S6 2.442(8) 3_656 ?
Sb2 S3 2.517(9) 3_656 ?
Sb2 S5 2.700(9) 3_656 ?
Sb2 S4 2.702(8) . ?
As1 S5 2.253(9) 4_566 ?
As1 S2 2.295(9) 3_656 ?
As1 S3 2.334(9) 4_566 ?
As2 S8 2.289(9) . ?
As2 S7 2.301(9) 3_756 ?
As2 S4 2.313(9) 3_656 ?
S1 Sb1 2.494(8) 1_455 ?
S1 Sb1 2.586(8) 3_655 ?
S2 As1 2.295(8) 3_656 ?
S2 Pb2 3.068(8) 3_656 ?
S3 As1 2.334(9) 4_565 ?
S3 Sb2 2.517(9) 3_656 ?
S4 As2 2.313(9) 3_656 ?
S5 As1 2.253(9) 4_565 ?
S5 Sb2 2.700(9) 3_656 ?
S6 Sb2 2.442(8) 3_656 ?
S6 Pb1 2.968(8) 4_565 ?
S6 Pb2 3.104(8) 4_565 ?
S7 As2 2.301(9) 3_756 ?
S7 Sb1 2.868(8) 4_566 ?
S7 Pb2 2.911(7) 1_655 ?
S8 Pb1 3.001(8) 4_565 ?
S8 Pb2 3.058(8) 4_665 ?

loop_
 _geom_angle_atom_site_label_1
 _geom_angle_atom_site_label_2
 _geom_angle_atom_site_label_3
 _geom_angle
 _geom_angle_site_symmetry_1
 _geom_angle_site_symmetry_3
 _geom_angle_publ_flag
S4 Pb1 S6 71.0(2) . 4_566 ?
S4 Pb1 S8 75.5(2) . 4_566 ?
S6 Pb1 S8 89.8(2) 4_566 4_566 ?
S7 Pb2 S8 74.4(2) 1_455 4_466 ?
S7 Pb2 S2 134.2(2) 1_455 3_656 ?
S8 Pb2 S2 143.7(2) 4_466 3_656 ?
S7 Pb2 S6 68.0(2) 1_455 4_566 ?
S8 Pb2 S6 89.3(2) 4_466 4_566 ?
S2 Pb2 S6 84.6(2) 3_656 4_566 ?
S1 Sb1 S1 86.7(3) 1_655 3_655 ?
S1 Sb1 S2 94.7(3) 1_655 . ?
S1 Sb1 S2 92.2(2) 3_655 . ?
S1 Sb1 S7 79.2(2) 1_655 4_565 ?
S1 Sb1 S7 163.3(2) 3_655 4_565 ?
S2 Sb1 S7 80.2(2) . 4_565 ?
S6 Sb2 S3 93.1(3) 3_656 3_656 ?
```

```
S6 Sb2 S5 94.8(3) 3_656 3_656 ?
S3 Sb2 S5 81.8(3) 3_656 3_656 ?
S6 Sb2 S4 91.0(3) 3_656 . ?
S3 Sb2 S4 85.9(3) 3_656 . ?
S5 Sb2 S4 166.7(3) 3_656 . ?
S5 As1 S2 98.0(4) 4_566 3_656 ?
S5 As1 S3 96.3(3) 4_566 4_566 ?
S2 As1 S3 96.9(3) 3_656 4_566 ?
S8 As2 S7 96.5(3) . 3_756 ?
S8 As2 S4 96.7(3) . 3_656 ?
S7 As2 S4 100.6(3) 3_756 3_656 ?
Sb1 S1 Sb1 93.3(3) 1_455 3_655 ?
As1 S2 Sb1 97.1(3) 3_656 . ?
As1 S2 Pb2 107.4(3) 3_656 3_656 ?
Sb1 S2 Pb2 90.6(3) . 3_656 ?
As1 S3 Sb2 92.3(3) 4_565 3_656 ?
As2 S4 Sb2 108.5(3) 3_656 . ?
As2 S4 Pb1 99.5(3) 3_656 . ?
Sb2 S4 Pb1 97.6(2) . . ?
As1 S5 Sb2 89.5(3) 4_565 3_656 ?
Sb2 S6 Pb1 103.7(3) 3_656 4_565 ?
Sb2 S6 Pb2 107.8(3) 3_656 4_565 ?
Pb1 S6 Pb2 88.2(2) 4_565 4_565 ?
As2 S7 Sb1 93.7(3) 3_756 4_566 ?
As2 S7 Pb2 101.4(3) 3_756 1_655 ?
Sb1 S7 Pb2 164.8(3) 4_566 1_655 ?
As2 S8 Pb1 101.1(3) . 4_565 ?
As2 S8 Pb2 98.9(3) . 4_665 ?
Pb1 S8 Pb2 90.5(2) 4_565 4_665 ?

_diffrn_measured_fraction_theta_max    0.893
_diffrn_reflns_theta_full              20.91
_diffrn_measured_fraction_theta_full   0.893
_refine_diff_density_max    1.827
_refine_diff_density_min   -1.750
_refine_diff_density_rms    0.357
```